Journal Article

Pomegranate seed oil stabilized with ovalbumin glycated by inulin: Physicochemical stability and oxidative stability

Han, L., Wang, K., Hu, B., Zhou, B., Yang, J. and Li, S.

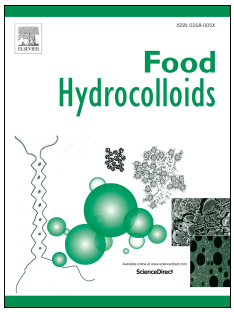

Pomegranate seed oil stabilized with ovalbumin glycated by inulin: Physicochemical stability and oxidative stability

Lingyu Han, Kangping Wang, Bing Hu, Bin Zhou, Jixin Yang, Shugang Li

PII: S0268-005X(19)32068-5

DOI: https://doi.org/10.1016/j.foodhyd.2019.105602

Reference: FOOHYD 105602

To appear in: *Food Hydrocolloids*

Received Date: 8 September 2019

Revised Date: 20 November 2019

Accepted Date: 12 December 2019

Please cite this article as: Han, L., Wang, K., Hu, B., Zhou, B., Yang, J., Li, S., Pomegranate seed oil stabilized with ovalbumin glycated by inulin: Physicochemical stability and oxidative stability, *Food Hydrocolloids* (2020), doi: https://doi.org/10.1016/j.foodhyd.2019.105602.

Author Statement

We confirm that the manuscript, or its contents in some other form, has not been published previously by any of the authors and/or is not under consideration for publication in another journal at the time of submission. All authors have seen the manuscript and approved to submit to your journal. Thank you very much for your attention and consideration.

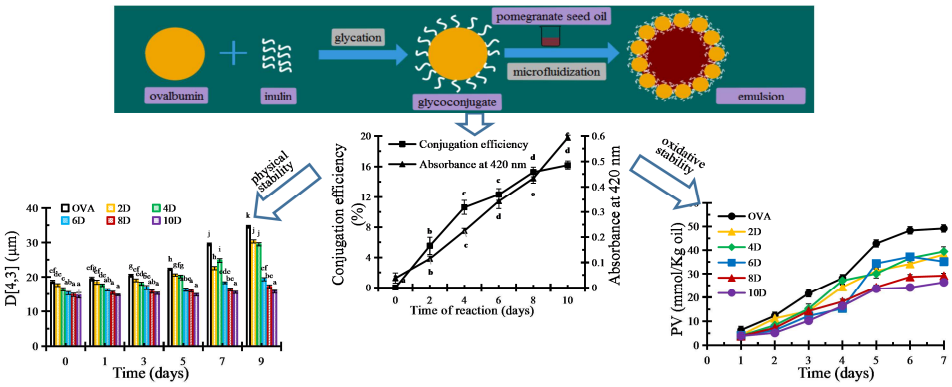

Pomegranate seed oil stabilized with ovalbumin glycated by inulin: Physicochemical stability and oxidative stability

Lingyu Han‡[a,b], Kangping Wang‡[a], Bing Hu[a], Bin Zhou[a], Jixin Yang[c], and Shugang Li[a]*

[a] Key Laboratory of Fermentation Engineering, Ministry of Education; Glyn O. Phillips Hydrophilic Colloid Research Center, School of Bioengineering and Food, Hubei University of Technology, Wuhan, 430068, China

[b] Key Lab of Biotechnology and Bioresources Utilization of Ministry of Education, College of Life Science, Dalian Minzu University, Dalian, Liaoning, 116600, China

[c] Faculty of Arts, Science and Technology, Wrexham Glyndwr University, Plas Coch, Mold Road, Wrexham, LL11 2AW, United Kingdom

*Corresponding author: Prof. Shu-gang Li,.

E-mail: lishugang2010@163.com. +86-27-59750467

‡ These authors contributed equally to this work.

Key words: pomegranate seed oil emulsion, ovalbumin, inulin, glycation, stability

Abstract

Pomegranate seed oil is rich of conjugated fatty acids which are highly appealing for a variety of applications in food industry. In this research, ovalbumin (OVA) and ovalbumin-inulin glycoconjugates with different Maillard reaction times were used to stabilize pomegranate seed oil emulsions and their impact on physicochemical stability and oxidative stability of the products was investigated. The OVA-inulin glycoconjugate produced on 10th day of Maillard reaction has exhibited significantly higher conjugation efficiency, lower surface hydrophobicity and lower surface tension than other glycoconjugates. The secondary conformation of OVA and conjugates determined by far-UV circular dichroism spectroscopy has remarkably changed. The reduction in intensity of Trp-fluorescence observed in glycated proteins with inulin indicated that the glycation affected partially the side chains of protein in tertiary structure through the Maillard reaction without great disruption of native structure. The emulsion stabilized by OVA-inulin glycoconjugate obtained by 10 days Maillard reaction has shown the best physicochemical stability. Compared with the OVA emulsion, the oxidative stability of the glycated OVA emulsion system was significantly improved ($p < 0.05$). Fatty acid profile results also confirmed that OVA-inulin glycoconjugates were able to prevent the pomegranate seed oil from oxidation. It is suggested that the inulin attached to OVA by glycation played a vital role in physicochemical stability and oxidative stability of pomegranate seed oil emulsions.

1. Introduction

Pomegranate seed oil is rich of conjugated fatty acids (around 65-80% in weight), among which conjugated linolenic acid stands out because of its chemical construction (Abbasi, Rezaei, & Rashidi, 2008; Sassano et al., 2010). Its bioactivity is related to the inhibition of certain types of cancer, modulation of the immune system, and reducing the risks of obesity and cardiovascular diseases (Hennessy, Ross, Devery, & Stanton, 2011; Saha, Chakraborty, Ghosh, & Ghosh, 2012). Besides, tocopherols and phytosterols can be found in pomegranate seed oil (Goula, Papatheodorou, Karasavva, & Kaderides, 2016). They may be able to regulate oxidative stress and inflammation, leading to reduced risk of various chronic diseases (Aslani & Ghobadi, 2016; Zhang & Rong, 2016). Pomegranate seed oil has been well developed for antioxidant properties, activity of antioxidant enzymes, immune function, lipid metabolism, and other potential health benefits (Meerts et al., 2009; Tong, Kasuga & Khoo, 2006; Yamasaki et al., 2006).

There has been growing interest in producing foods from pomegranate seed oil instead of using pomegranate seeds as animal feed or in cosmetic products. However, some environmental conditions, such as light, temperature, oxygen, humidity, *etc.* could cause oxidation of unsaturated fatty acids and other unwanted reactions (Yekdane & Goli, 2019). Emulsion of pomegranate seed oil has proven to be an efficient way to protect and deliver unsaturated fatty acids in foods. The key factor of pomegranate seed oil emulsion was to choose emulsifiers which would affect its stability. Good emulsifiers could quickly adsorb to the surface of oil droplets, forming a coating layer against aggregation and coalescence (Liu et al., 2019). The glycated food proteins after Maillard reaction could achieve a better emulsion stability compared to the unmodified proteins, which has been well researched (An et al., 2014; Chen et al., 2016).

Ovalbumin (OVA) is a main constitute from egg white proteins, which has demonstrated emulsifying ability and been most widely used as a model protein (Ma, Gao, & Chen, 2013). However, due to its poor stability, the oil-in-water emulsion prepared by OVA is not able to effectively prevent pomegranate seed oil from oxidation. Therefore, different efforts have been made to improve the stability of OVA emulsions, among which the Maillard reaction with protein is seen as the most

promising one (Ozturk & McClements, 2016). In this study, we performed the glycosylation of OVA with inulin which is considered to be a stabilizer for emulsions (López-Castejón et al., 2019). Inulin is a fructan consisting almost entirely of linear beta-1,2-linked fructose units with a terminal alpha1-beta2-linked glucose molecule, presented in many plant species such as Jerusalem artichoke, dahlia and chicory root, or synthesized products from sucrose (Schaafsma & Slavin, 2015). The aim of this research was to determine the impact of OVA-inulin glycoconjugates on the pomegranate seed oil-in-water emulsions. In particular, we would elucidate the contribution of inulin (through Maillard reaction) to the antioxidant function by analyzing radical scavenging activity and lipid oxidation in the pomegranate seed oil in water emulsions.

In this work, oil-in-water emulsions were prepared by OVA and OVA-inulin glycoconjugates with different reaction times to protect the nutritional value of pomegranate seed oil. The physicochemical stability of pomegranate seed oil emulsions was analyzed through droplet size distribution, zeta-potential, hydrodynamic diameters and interfacial surface tension. Furthermore, DPPH· radical scavenging activity, peroxide value determination and fatty acid profile composition analysis were used to evaluate the oxidation stability of pomegranate seed oil emulsions. The results of this research might suggest the 10D emulsifier (the sample obtained after 10 days of Maillard reaction) has shown the best ability for stabilization of pomegranate seed oil quality, and provided the technical support for industrial application of Maillard reaction products.

2. Material and methods

2.1 Materials.

High-performance inulin (degree of polymerization＜10, Chicory) was supplied by FANINON (Qinghai, China). Albumin Egg (A-5253), under the commercial name of Sigma, was purchased from Sigma-Aldrich, and pomegranate seed oil with 98% purity was purchased from ZETONG (Xi'an, China). 1,1-diphenyl-2-picrylhydrazyl (DPPH) was purchased from Aladdin Reagent Co. (Shanghai, China). Ammonium

thiocyanate, o-phthalaldehyde "Space" (OPA) and L-2-Amino-iso-hexanoic acid (≥ 99%) were purchased from Macklin Biochemical Technology Co. (Shanghai, China). Other chemicals were purchased from Sinopharm Chemical Reagent Co., Ltd (Shanghai, China).

2.2 Preparation of OVA-inulin glycoconjugates.

OVA-inulin glycoconjugates were prepared according to the method published by An et al. (2014). Briefly, OVA was dissolved in 100 mL of phosphate buffer (0.05 mM, pH 7.0). Inulin (0.25 g) was added into the OVA solution with stirring until it was fully dissolved, and then the mixture was lyophilized in a freeze-dryer (FD-1C-50, Beijing, China). The dried powders were incubated at 60 ℃ and 79% relative humidity in a SPX-150B-Z incubator (Shanghai, China) and samples were collected after 2, 4, 6, 8 and 10 days. OVA-inulin glycoconjugates with different reaction times were obtained by dialyzing 3 days with 7 kDa dialysis bag, and were named 2D, 4D, 6D, 8D and 10D, respectively, sealed and stored at -20 ℃ before use.

2.3 OVA-inulin glycoconjugates characterization.

2.3.1 FTIR.

FTIR spectra of OVA and OVA-inulin samples were measured using the method as previously reported (Han, Ratcliffe, & Williams, 2017). The sample was mixed with potassium bromide (KBr) at a mass ratio of 1:250, and then pressed and subjected to Fourier transform infrared spectroscopy (FTIR). Spectra were obtained from 64 scans at a resolution of 4 cm^{-1} from a potassium bromide sample pan in a range of 4000 cm^{-1} to 400 cm^{-1} by using a Perkin Elmer Spectrum RXI FT-IR spectrometer (Perkin Elmer Instruments, Massachusetts, USA).

2.3.2 Conjugation efficiency.

The conjugation efficiency was determined, according to Davidov-Pardo et al. (2015), by measuring the reduction in free amino groups using the OPA. The OPA reagent was freshly made prior to use. In brief, 40 mg OPA (dissolved in 1.0 mL 95% ethanol v/v), 25 mL sodium tetraborate buffer (pH 9.5), 2.5 mL SDS solution (w/v),

and 0.10 mL 2-mercaptoethanol were mixed together and then topped up to 50 mL with deionized water. Then, 0.05 mL of the 5 mg/mL conjugate solution was blended with 1.35 mL OPA reagent and incubated for 1 min at room temperature. The absorbance of obtained solution was measured immediately at 340 nm using a TU-1900 UV-VIS spectrophotometer (Beijing, China). Calibration curves were constructed using L-leucine (1-5 mM) as a standard compound containing an amino group. The following equation was used to define the conjugation efficiency.

$$\text{Conjugation efficiency (\%)} = \left(1 - \frac{\text{amine groups after conjugation (M)}}{\text{amine groups before conjugation (M)}}\right) \times 100 \qquad (1)$$

2.3.3 Color measurement.

The brown color solution of glycated OVA (10 mg/mL) was analyzed by measuring the absorbance at 420 nm using a UV-visible spectrophotometer (TU-1900, Beijing).

2.3.4 Surface hydrophobicity (H_0).

The H_0 values of OVA and OVA-inulin glycoconjugates were determined according to Shah, Umesh, & Singhal (2019) using the hydrophobic fluorescence probe with 8-Anilino-1-naphthalenesulfonic acid (ANS). The sample solution (1 mg/mL) was diluted to 0.00125, 0.0025, 0.005, 0.01, 0.02 mg/mL, respectively. 4 mL sample solution was mixed with 20 μL of 8 mM ANS solution. The fluorescence intensity of the mixed solution was detected at excitation wavelength 390 nm and emission wavelength 470 nm using an F-4600 luminescence spectrophotometer (Hitachi High-Technologies Corporation, Hitachi, Japan). The H_0 of samples was determined by the slope of the relative fluorescence (R) versus the percent protein concentration (w/v).

2.3.5 Circular dichroism (CD) spectroscopy.

The sample solutions (0.2 mg/mL) were analyzed by a Jasco J-1500 spectropolarimeter (Jasco, Japan) and scanned from 190 to 250 nm at 25 □. Each spectrum was an average of three scans to reduce noise before structural analysis was performed.

2.3.6 Fluorescence spectroscopy.

Fluorescence analysis of OVA and OVA-inulin glycoconjugates was performed according to Li et al. (2009) using a fluorescence spectrometer (Hitachi High-Technologies Corporation, Hitachi, Japan).

2.3.7 Particle size and zeta potential

The mean particle diameter, polydispersity index, and particle size distribution based on number were obtained using a dynamic light scattering instrument (Zetasizer 3000, 174 Malvern Instruments, Malvern, UK) according to the pervious method (Han, Ratcliffe, & Williams, 2015). The hydrodynamic diameter was obtained from the Stokes-Einstein relationship using the instrument software. The zeta potential of samples was determined using particle electrophoresis by the same equipment. The samples were diluted 20 times to avoid multiple scattering effects and equilibrated at 25 ˚C prior to analysis.

2.3.8 Surface tension measurements.

The interfacial adsorption of OVA and OVA-inulin glycoconjugates at the oil-water interface changing with time was measured by a TRACKER drop profile tensiometer (Teclis Tracker, France) using the method previously reported (Hu et al., 2019). The experiments were carried out at 25 ± 1°C. Evaporation of the aqueous phase into air caused a reduction of the drop volume at the water/air interface. The total experimental duration was set as 7200 s.

2.3.9 DPPH· radical scavenging assay

The DPPH· radical scavenging activity of OVA and OVA-inulin glycoconjugates was evaluated according to Chang et al. (2017). 3 mL sample solution was mixed with 1 mL of 0.1 mM DPPH methanol solution. After 30 min of reaction in darkness at room temperature, the mixture was centrifuged at 4000 g for 5 min to remove insoluble aggregates. A was referred to the absorbance of the supernatant measured at 517 nm; and A_0 was referred to the absorbance of 3 mL of H_2O mixed with 1 mL DPPH solution. The following equation was used to calculate the DPPH· radical-scavenging activity:

$$\text{DPPH}\cdot \text{ radical scavenging activity} = (A_0 - A)/A_0 \times 100\% \quad (2)$$

2.4 Preparation of pomegranate seed oil in water emulsions.

Six aqueous phases were prepared by dissolving 0.6 g sample (OVA, 2D, 4D, 6D, 8D, 10D) in 39.4 mL distilled water in six 100 mL tubes, respectively. 10 g pomegranate seed oil was added in each of these 6 tubes to make 20% oil-in-water emulsions. Emulsification was achieved using an IKARO10 Digital Ultra-Turraxhomogensier at 19000 rpm for 2 min.

2.5 Physicochemical stability of pomegranate seed oil emulsions by OVA-inulin glycoconjugates.

2.5.1. Droplet size distribution measurement

To evaluate the properties and stability of samples, the droplet size distribution of pomegranate seed oil emulsions was determined using a laser diffraction technique (Master-Sizer 2000, Malvern Instruments Ltd.) according to the literature (Han, Ratcliffe, & Williams, 2015) and the particle size was given as the volume-weighted mean diameter (D [4, 3]).

2.5.2 Influence of ionic strength and pH

The emulsifying properties of pomegranate seed oil emulsions by OVA-inulin glycoconjugates under different ionic strengths and pH conditions were also investigated. NaCl solution (0–250 mM) was added to the pomegranate seed oil emulsions. In addition, the pHs of fresh emulsions were adjusted to 3, 5, 7 and 9, respectively, using 0.1 M HCl or 0.1 M NaOH. The pomegranate seed oil emulsions were then stored at 25 ± 1°C for 24 h prior to the zeta potential and droplet size distribution analyses.

2.5.3 Peroxide value determination

Lipid hydroperoxides were measured as the primary oxidation products using a method adapted from Liu et al. (2019). 0.3 mL emulsion was added to 1.5 mL of a mixture of isooctane/2-propanol (3:1, v/v) , vortexed shock three times for 10 s each and centrifugated at 10,000 g for 2 min. 0.2 mL of the organic phase was added to a mixture of methanol/butanol (2:1, v:v) followed by 15 μL of 3.94 M thiocyanate and 15 μL of 0.072 M Fe^{2+} and the mixture was vortexed for 20 min.

Its absorbance was measured at 510 nm using a TU-1900 UV-visible spectrophotometer (Beijing, China). The concentration of hydroperoxides was calculated from a cumene hydroperoxide standard curve.

2.5.4 Fatty acid profile

The GC–MS analysis of pomegranate seed oil was performed according to Wang et al. (2014). The experiment was performed using an Agilent 7890B/5977A/7693 Autosampler Series Gas Chromatograph (Agilent Technologies, Palo Alto, CA) using a DB-WAX capillary column (30 m × 0.25 mm × 0.25 mm film thickness, Hewlett Packard, USA).

2.5.5 Confocal laser scanning microscopy analysis (CLSM)

Microstructural analysis of emulsions was implemented using a Leica TCS SP8 Confocal Laser Scanning Microscope (Leica Microsystems, Mannheim, Germany) as observed by Frederico et al. (2018). 10 μL of Nile Red and 10 μL of Nile Blue, dissolved in ethanol (1 mg/mL), were mixed into 1 mL of emulsions to stain oil drops and emulsifiers, respectively. The excitation spectra of Nile Red and Nile Blue were measured at 488 nm and 633 nm, respectively. All images were taken using simultaneous dual-channel imaging. At least three specimens of each sample were observed to obtain representative micrographs of samples.

2.5.6 Transmission electron microscopy (TEM) observation

To further evaluate the physical protective action of conjugates in emulsion, TEM images of the emulsions (OVA, 2D, 4D, 6D, 8D and 10D) were observed using a transmission electron microscopy (Tecnai G_2 20, Hillsboro, USA) operating at an acceleration voltage of 80 kV. The TEM analysis of pomegranate seed oil emulsions was performed according to Pan et al. (2019). One drop of emulsions and one drop of phosphotungstic acid (1%, m/v) were mixed and placed on a copper grid of 200 meshes for 1 min.

2.6 Statistic analysis

Statistical analysis was carried out using SPSS 23.0 (SPSS Inc., Chicago, IL). Data were shown as mean ± S.D. (n=3). Differences between means of each group were

assessed using one-way analysis of variance followed by Duncan's test. Significant differences were accepted as a P-value < 0.05.

3. Results and discussion

3.1 FTIR spectra

FTIR spectra of OVA and OVA-inulin glycoconjugates have been researched in this study. The peaks for OVA at 1753 cm^{-1} (amide Ⅰ) and 1615 cm^{-1} (amide Ⅱ) indicate C=O stretching and N-H stretching, respectively (Chen et al., 2016). The broad band observed in the 3500-3000 cm^{-1} range is attributable to free and bound O-H and N-H groups, which are able to form hydrogen bonding with the carbonyl group of the peptide linkage in proteins (Sheng et al., 2014). The intensities of -C-O stretching and -OH deformation vibrations at 1050-1150 cm^{-1} in the OVA-inulin conjugates increased, while the peak at 1754 cm^{-1} decreased compared with native OVA, indicating that partial amine groups were consumed by Maillard reaction and the saccharides were linked to OVA through covalent bonds (Sugumaran et al., 2013).

3.2 Characterization of OVA glycated by inulin

There are two factors to assess the glycosylation development: conjugation efficiency and a brown color solution (Bi et al., 2017). The conjugation efficiency of the glycoconjugates was determined using the OPA. As shown in Figure 1a, the conjugation efficiencies of five glycoconjugates (2D, 4D, 6D, 8D, 10D) were 5.54±1.14%, 10.61±0.93%, 12.32±0.77%, 15.28±0.63%, and 16.19±0.52%, respectively. It was found that the conjugation efficiency of OVA was significantly increased with the reaction period of time, which suggests that OVA glycated with inulin through Maillard reaction more violently with prolonged reaction time. Glycation was accompanied by a browning coloration. From the present research, the brown color was originated from the secondary Marillard reaction products. The 420 nm absorption spectra obtained for OVA-inulin glycoconjugates during different reaction times are also shown in Figure 1a. With an increase in reaction time, the absorbance of five glycoconjugates at 420 nm also increased. Clearly, the reaction

rate in the OVA-inulin glycoconjugates was proportional to the conjugation efficiency during Marillard reaction.

There is a strong correlation between surface hydrophobicity of a protein and its functional properties, such as emulsifying property, foam stability, and fat binding capacity (Liu et al., 2019). The effect of glycation treatment on the conformational state of modified OVA was evaluated by H_0. The results from Figure 1b show that H_0 of glycated OVA incubated for 2 days slightly increased compared to the native OVA. It was probably related to the exposure of hydrophobic patches on the protein surface, and the results reported by Liu et al. (2017) also found the same slight increase (Corzo-Martínez, Moreno, Olano, & Villamiel, 2008). With the increase in incubation time (4-10 days), H_0 of different glycated OVAs was significantly decreased compared to the native OVA, which implies that the presence of hydrophilic cluster molecules on the surface of glycated OVAs was reduced. It might be due to that hydrophobic amino acids of protein, such as proline, leucine, and valine, as well as cationic groups in lysine and/or arginine, were blocked by dextrans in the glycoconjugates. Meanwhile, ANS may also strongly bind with cationic groups of protein (Liu et al., 2012). In addition, the difference in conjugation efficiency might be another reason to affect the H_0 difference in the glycoconjugates.

Surface tension kinetics for OVA and OVA-inulin glycoconjugates with different reaction times up to 7200 seconds are shown in Figure 2. There was a sharp decrease in surface tension during the first 500 seconds, while it tended to become a steady state with a relatively more gradual decrease in surface tension after 1000 seconds. Then the surface tension was maintained as a uniform value after 3000 seconds. It can be seen clearly that OVA showed the highest surface tension, and the order of it for the OVA-inulin glycoconjugates with different reaction times was as follow: 2D> 4D > 6D > 8D > 10D. This was demonstrated by the final surface tension values (at 7200 s) of 42.28±0.077 mN/m, 38.83±0.096 mN/m, 39.33±0.055 mN/m, 36.09±0.154 mN/m, and 34.06±0.077 mN/m for OVA, 2D, 4D, 6D, 8D and 10D, respectively. These results indicate that, with extending the reaction time, the ability of decreasing the surface activity by OVA-inulin glycoconjugates was enhanced compared to the native OVA. This is also certified by the surface hydrophobicity values (Figure 1b) where 10D was the least hydrophobic and H_0 of different glycated OVAs significantly decreased compared to the OVA with the increase in reaction time. This is consistent

with the study by Liu et al. (2019). The surface activity of proteins was improved because of glycation with a hydrophobic group rather than a hydrophilic group (Rangsansarid et al. 2008). In this study, the hydrophilic hydroxyl groups from inulin lowered the surface activity of OVA. With the reaction time increasing, the conjugation efficiency (Figure 1a) also increases, which means the OVA-inulin glycoconjugates reduced the surface activity of OVA to more and more extent. Some previous studies have also shown that glycation with glucose led to more rapid adsorption (Zhu, Wang, & Zhao, 2017; Liu et al., 2019). The increased surface interfacial activity would lead to improved emulsification properties (Kristinsson & Hultin, 2003).

The secondary structural composition for native OVA was approximately as follows: 38.2% α-helix; 16.85% β-sheet; 16.1% Turn; and 28.9% random coil (Table 1), calculated by the CONTIN/LL program in CD Pro software. There was a general tendency of negative and positive band shifts to lower wavelength because of the glycation, and the negative ellipticity of these bands considerably decreased with the reaction time compared to native OVA, indicating that the secondary conformation was distinctly changed by the treatment. In addition, in the dry state, each protein molecule unreacted in the reaction period was in close contact with neighboring molecules forming intermolecular hydrogen-bonded β-sheets. The increased inter-molecular interactions among the neighboring proteins possibly led to an increase in the amount of intermolecular β-sheets and naturally a decrease in α-helix and random coil (Figure 2b and Table 1).

Trp-fluorescence is a common index used to detect the changes of protein conformation and amino acid (Sun et al. 2004). Changes of the native OVA and glycated OVAs in Trp-related fluorescence were observed by fluorescence emission spectra following an excitation at 280 nm (Figure 2c). In the results of OVA-inulin conjugates, the Trp-fluorescence was lower than that of native OVA, where the fluorescence intensity of native OVA (514.16) is approximately 3 times of that (157.49) of OVA-inulin conjugates when incubated for 10 days. It might be due to the shielding effect of the carbohydrate bound (Liu et al. 2017). The reduction in intensity of Trp-fluorescence observed in glycated proteins with inulin indicates that the glycation affected partially the side chains of protein in its tertiary structure through the Maillard reaction without great disruption of native structure (Sun et al. 2004).

Similar findings were achieved with OVA (Sun et al. 2004), phaseolin (Tang et al. 2011), and silver carp myosin (Liu et al. 2017) during glycation.

Figure 2d shows apparent mean zeta potentials of OVA and OVA-inulin glycoconjugates as a function of pH. The total biopolymer concentration was 0.1% (w/w). The native OVA solution had an isoelectric point (IEP) of 4.70 which was corresponding to the literature value 4.75 (Chen et al., 2018). The strongest reduction of IEP was observed for the OVA-inulin incubated for 10 days, which was down to around 4.10. Meanwhile, it can be seen that with the increase in reaction time, the IEP decreased for the OVA-inulin glycoconjugates and their IEP values were lower than that of the native OVA. It was possibly attributed to the glycation with dextran reducing the amount of ionizable amino groups on the OVA (Liu et al., 2019).

The antioxidant activity of modified complexes was characterized by measuring the free radical scavenging rate (Habinshuti et al., 2019; Nooshkam et al., 2019). The DPPH· radical scavenging activity of glycated OVAs is shown in Figure 3. The results show a tendency that with the increase of reaction time, the DPPH· radical scavenging activity of glycated OVAs was significantly improved ($P > 0.05$). The DPPH· radical scavenging rate of native OVA solution was 21%, but after the OVA-inulin glycoconjugates were incubated for 2, 4, 6, 8 and 10 days, the DPPH· radical scavenging rates were 27.5%, 48%, 62%, 80%, and 84%, respectively. The Maillard reaction is a chemical method that has been proposed to improve the free radical scavenging activity, which could be partially related to the caramelization of glucose (Liu et al., 2012). According to Wooster et al. (2006), during the Maillard reaction, a series of substances with strong antioxidant activity, which include reducing ketones, melanoids and some small volatile heterocyclic compounds, are produced. As shown in Figure 1a, at reaction time up to 8 days or 10 days, there was no significant change to the DPPH· radical scavenging activity ($P > 0.05$), which indicates the upper limit of inhibiting oxidation.

3.3 The kinetics of adsorption

In order to determine the dynamic adsorption of OVA and OVA-inulin glycoconjugates at the oil-water interface, 0.1% (w/w) OVA or OVA-inulin glycoconjugate solution was used as the aqueous phase and the oil phase was pomegranate seed oil. The dynamics of OVA and OVA-inulin glycoconjugates

adsorption at the pomegranate seed oil–water interface were examined over the time scale ranging from seconds to several hours by measuring the interfacial tensions at 25 °C (Figure 4). It has been clearly observed that the interfacial tension decreased progressively along with the adsorption time, with faster changes at earlier adsorption period indicating that there was a spontaneous adsorption of OVA and OVA-inulin glycoconjugates at the interface. After the interface was formed, the decrease was initially steeper followed by an asymptotical plateauing. This shape was characteristic for the interfacial tension evolution of the emulsifier laden oil/water interface. Meanwhile, the initial interfacial tension of OVA-inulin glycoconjugates was significantly lower than that of OVA, indicating that the adsorption rate of OVA-inulin glycoconjugates at the pomegranate seed oil–water interface increased with longer reaction time. It was the conjugation efficiency that affected the ability of interfacial adsorption. The time required for reducing interfacial tension by 30% of the initial value at the pomegranate seed oil–water interface due to the adsorption of OVA and OVA-inulin glycoconjugates and the equilibrium interfacial tension at 7200 s at 25 °C are shown in Table 2. The interfacial tension of OVA-inulin glycoconjugates showed more rapid adsorption compared to the native OVA and better ability to reduce the equilibrium interfacial tension. It indicated that the adsorption rate of OVA-inulin glycoconjugates increased with the incubation time. It might be due to that the surface hydrophobicity (Figure 1b) and zeta potential (Figure 3d) of OVA-inulin glycoconjugates decreased with the reaction time. Hence there are many factors to be considered which may affect the adsorption rate among the different emulsifiers such as: emulsifier size, hydrophobicity, instability, charge and disulfide bond (Hu et al., 2019).

3.4 Physicochemical stability of pomegranate seed oil emulsions stabilized by glycated OVA

Emulsions are thermodynamically unstable systems with the possibilities of creaming, flocculation and coalescence (Schroder et al., 2017). The droplet size distribution and volume mean diameter (D[4,3]) of the freshly prepared 20% pomegranate seed oil emulsions stabilized by OVA and OVA-inulin glycoconjugates were measured to evaluate their emulsion stability at 60□ (Figure 5a and 5b). The

emulsions contained 1.2% OVA or glycated OVA with 20% pomegranate seed oil as mentioned in the experimental section. The droplet size distribution of the emulsions stabilized by OVA and OVA-inulin (2D) showed almost no change during the first 3 days; and neither did the emulsions formed by 4D and 6D after storing 5 days at 60 □. The size distribution of the emulsion stabilized by 10D stayed the same over 9 days at 60 □ which was the best one. These emulsions had different droplet sizes, where the smallest droplet size ($d \approx 14.0$ μm) emulsion was made by 1.2% glycated OVA (10D) and the biggest one ($d \approx 18.0$ μm) was made by 1.0% native OVA. All the glycated OVAs (OVA-inulin) have formed a smaller size emulsion ($P < 0.05$) compared to the one made by native OVA. Noticeably, no significant ($P > 0.05$) change was observed in the volume mean diameter D [4,3] for accelerated emulsion formed by 10D during storage time up to 9 days, indicating its high stability against coalescence. The better storage stability was attributed to smaller droplet size (Liu et al., 2019), which is due to the adsorption ability at the oil-water interface. The strong emulsifiers could rapidly adsorb at the oil-water interface to lower the interfacial tension then form a smaller droplet. The data of interfacial tension (Figure 4) indicate the 10D could stabilize an emulsion with smallest droplets compared to other OVA-inulin emulsifiers with shorter incubation time. Visual observation of the emulsions prepared by OVA and glycated OVAs is shown in Figure 5c. OVA glycosylates with carboxymethyl cellulose of different substitution degrees also show a better emulsifying activity (Su et al., 2018).

The droplet sizes and zeta potentials of pomegranate seed oil emulsions with OVA and OVA-inulin glycoconjugates at different pHs are given in Figure 6a. At pH = 3 the zeta potentials with OVA and glycated OVAs were positive because the IEP were 4.70 for OVA and 4.50-4.10 (Figure 2d) for OVA-inulin glycoconjugates with different reaction times from 2 days to 10 days. The absolute value of glycated OVAs was significantly higher ($p < 0.05$) than that of OVA. Meanwhile, at pH 5-9 the zeta potentials of pomegranate seed oil emulsions with OVA and OVA-inulin glycoconjugates were negative and the absolute value was also significantly higher ($p < 0.05$) for OVA-inulins compared to the native OVA. The droplet size of the emulsions made by OVA-inulins decreased significantly ($p < 0.05$) with the reaction

time increasing, where the smallest size of pomegranate seed oil droplet was found in the emulsion stabilized by OVA-inulin with 10 days reaction. With increasing pH, the mean diameter of the emulsion formed with 10D decreased from 30 μm to 16 μm. It was due to that the electrostatic repulsive force between the oil bodies was weak when the pH was near the isoelectric point, which may weaken the stability of the emulsions at pH 3 and pH 5 according to the work of Su et al. (2018). The electrostatic and steric repulsion between the oil droplets increased because they were surrounded by a charged layer, concurrently reducing the van der Waals attraction (Lesmes et al., 2012). At pH 7 and pH 9, the mean diameter of pomegranate seed oil emulsions was relatively small, which could be attributed to the stronger electrostatic repulsion between the oil droplets that prevented their aggregation. Compared to the native OVA, the glycated OVA-inulins clearly show that coating the pomegranate seed oil droplets can greatly extend the range of pH values at which they remain stable and prevent their aggregation.

As shown in Figure 6b, the zeta potential absolute value of pomegranate seed oil emulsion stabilized by OVA remarkably decreased ($P < 0.05$) from -32 mV to -17.5 mV with the salt concentration up to 250 mM NaCl. It was due to the electrostatic screening effects of sodium ions (Xu et al., 2012). However, the OVA-inulins stabilized emulsion has shown no significant ($p > 0.05$) changes on their zeta potential values, which were relatively high at pH 7 away to IEP (4.50-4.10). Figure 6c shows that the mean diameter of pomegranate seed oil emulsions maintained the same trend as zeta potential. The droplet size dramatically ($P < 0.05$) increased from 18.5 μm to 22 μm with the salt concentration varying from 0 to 250 mM. However, there was no significant ($p > 0.05$) change on the mean diameter of the droplets for the OVA-inulin glycoconjugates formed emulsions. These results showed that the OVA-inulin glycoconjugates used as a layer to coat oil droplet greatly improved the salt stability of pomegranate seed oil emulsions, which may have important implications for their utilization in food products.

The peroxide value (PV) is an important indicator to judge the quality of oil, which mainly reflects the change of hydroperoxide content in oil (Soleimanian et al., 2018). As shown in Figure 7, lipid hydroperoxides were detected in the pomegranate seed oil emulsions stabilized by OVA-inulin glycoconjugates during storage at 25 ± 1 °C. The degree of oxidation of the emulsion gradually increased with the storage period extended. After 4 days, there was a difference in the PV of the OVA-inulin glycoconjugates with different conjugation efficiencies. The oxidation stability of the glycated OVA emulsion system was better than the OVA emulsion ($p < 0.05$), and with the reaction time increasing, the oxidative stability of the glycated OVA emulsions improved. The PV of the OVA emulsion was the largest, being 47.58 mmol/kg oil after storing over a week, while the PV of 10D emulsion was just up to 31.27 mmol/kg oil. It may be due to that the glycated OVAs adsorbed at the oil-water interface formed a dense physical barrier, which hindered the entry of free radicals into the interior of the emulsion droplets and slowed down the rate of lipid oxidation (Xie et al. 2019). Meanwhile, with the extension of reaction time, more sugar chains were covalently grafted with OVA molecules. The protein molecules adsorbed at the oil-water interface formed a viscoelastic protective film, and the sugar chains formed a spatial three-dimensional network structure on the outer side. It further increased the thickness and mechanical strength of the interface film and greatly improved the oxidation stability of the emulsion (Shi et al. 2019).

3.5 Fatty acid profile of pomegranate seed oil in the emulsion stabilized by OVA-inulin glycoconjugates

Pomegranate seed oil is particularly susceptible to oxidation because of high degree of unsaturation. Oil oxidation could influence fatty acid composition, and the changes of fatty acid class imply oil quality (Wang et al. 2007). The pomegranate seed oil fractions were determined from the fatty acid profiles obtained by GC-MS analysis (Table 3). It was possible to see that PUFAs represented content more than 83.2% of total fatty acids, linolenic C18:3 fraction being the major component (76.3% of total fatty acids). After storing a week at 60 °C, the total content of SFA in pomegranate

seed oil increased, and the total content of PUFA decreased, which reduced the overall unsaturation. Among all the emulsions, the emulsion stabilized by 10D showed the minimum change on the content of SFA and PUFA compared to the initial values, which were 10.8% and 81.5%, respectively. The change in UFA content was mainly caused by the change of C18:3. The content of C18:3 in pomegranate seed oil completely exposed to air was reduced by 8.1%, and the one in pomegranate seed oil in OVA emulsion was reduced by 7.2%. With reaction time increased, the content of C18:3 gradually decreased. However, the C18:3 of pomegranate seed oil in 10D emulsion only decreased by 3.2%, which was possibly the result of the oxidative cleavage of fatty acids during storage (Tironi et al. 2007). To some extent, the emulsion by OVA-inulin glycoconjugates would be able to prevent the pomegranate seed oil from oxidation, particularly the OVA-inulin with 10 days reaction time.

3.6 CLSM and TEM

CLSM micrographs (including red, green and overlap field) of fresh emulsions (OVA, 2D, 4D, 6D, 8D and 10D) were shown in Figure S_2. The green fluorescence resided in spherical droplets, whereas red fluorescence resided in emulsifiers, certifying the type of emulsions was oil-in-water. Compared to the emulsions stabilized by OVA-inulin glycoconjugates, the CLSM images of OVA emulsion indicated that the OVA was unevenly distributed in aqueous phase instead of being well adsorbed at the interface of emulsion. Interestingly, the red fluorescence around the oil droplets in images of 6D, 8D and 10D was a thin but compact layer, while that of 10D was thicker and more dense. Furthermore, the red fluorescence layer around the oil droplets in 2D and 4D was not as conspicuous as those of 6D, 8D and 10D. According to the previous study (Fernandes et al., 2017), emulsifying agents generally stabilize emulsions by forming a coating over oil droplets and, thus, preventing agglomeration and oxidation. The change of the spatial structure is due to the combination of OVA and inulin through the Maillard reaction, which can quickly adsorb on the surface of the oil droplets to form a film, making the particle size smaller and more uniform. Similar findings were achieved by whey protein

538 isolate-gum acacia conjugates (Chen et al. 2019), Pea protein isolate-gum (Zha et al.
539 2019), and soy protein isolate-maltose (Xu et al. 2019) during glycation.

540 As illustrated in TEM, the stability of emulsions against environmental stress and
541 lipid oxidation could be basically affected by the compactness and thickness of the
542 network structure around oil droplets. TEM was adopted to visualize the network
543 structure of emulsions (OVA, 2D, 4D, 4D, 6D, 8D and 10D) and the result was
544 presented in Figure S_3. The droplets in OVA showed the gauzy and discontinuous
545 interfacial film composed of peptides, which was related to the unwound and flexible
546 structure of OVA and the incomplete repulsion attraction equilibrium between the
547 side chains of peptides. A thick and continuous network structure was observed in the
548 interface of emulsions stabilized by 8D and 10D, and the compactness and
549 consecutiveness of network structure were relied on the conjugation efficiency and
550 adsorption capacity of OVA in conjugates. As shown in OVA-inulin glycoconjugates
551 (2D,4D,6D,8D and 10D), the interfacial layer in 2D and 4D appeared loose and
552 discontinuous, while a tight cross-linked network structure around oil droplets in 8D
553 and 10D were observed, which contained the OVA with high conjugation efficiency
554 (Shi et al. 2019). The thickness and compactness of interfacial film were decisive not
555 only to the intensity of electrostatic forces, but also to the magnitude of steric
556 repulsion. The enhancement in the stability of emulsions stabilized by conjugates
557 (especially 10D) was primarily ascribed to the thickness and compactness of
558 interfacial layer around oil droplets, which acted as physical barrier to provide great
559 steric hindrance, and restrain the diffusion and infiltration of transition metal ions and
560 oxidation initiators into oil droplets to ameliorate the oxidative stability of emulsions.

561

562 **4. Conclusion**

563 Overall, the excellent storage stability and physical stability against environment
564 stress exhibited in pomegranate seed oil emulsions stabilized by OVA-inulin
565 glycoconjugates, which were attributed to the combined action of stabilization

emulsifiers (formed by the Maillard reaction of OVA with inulin) and increasing adsorption rate. The OVA-inulin glycoconjugates' DPPH • radical scavenging rate of the polymer increased and the peroxide value of the pomegranate seed oil emulsions grew slowly during storage, indicating that the emulsion prepared by the OVA-inulin glycoconjugates could effectively delay the pomegranate seed oil oxidation and protect its quality. CLSM and TEM further showed the Maillard reaction between OVA and inulin significantly improved the emulsifying properties of OVA. In particular, the 10D emulsion had the best stability. This study provides a promising approach to add value to the protection of pomegranate seed oil and OVA applications.

Acknowledgement

The work is funded by the National Key Research and Development Program of China (2018YFD0400302)，the grants from the National Natural Science Foundation of China (No. 31701555)，the National Public Welfare Industry (Agriculture) Special: Comprehensive Benefits of Processing Sub-Products of Horticultural Crop Products (No. 201503142-08)

References：

Abbasi, H., Rezaei, K., & Rashidi, L. (2008). Extraction of essential oils from the seeds of pomegranate using organic solvents and supercritical CO_2. *Journal of the American Oil Chemists Society, 85*(1), 83-89.

An, Y., Cui, B., Wang, Y., Jin, W., Geng, X., Yan, X., & Li, B. (2014). Functional properties of ovalbumin glycosylated with carboxymethyl cellulose of different substitution degree. *Food Hydrocolloids, 40*, 1-8.

Aslani, B. A., & Ghobadi, S. (2016). Studies on oxidants and antioxidants with a brief glance at their relevance to the immune system. *Life Sciences, 146*, 163-173.

Bi, B., Yang, H., Fang, Y., Nishinari, K., & Phillips, G. O. (2017). Characterization and emulsifying properties of β-lactoglobulin-gum Acacia Seyal conjugates prepared via the Maillard reaction. *Food Chemistry,* 214, 614-621.

Chang, C., Li, X., Li, J., Niu, F., Zhang, M., Zhou, B., Su, Y., & Yang, Y. (2017). Effect of enzymatic hydrolysis on characteristics and synergistic efficiency of pectin on emulsifying properties of egg white protein. *Food Hydrocolloids, 65,* 87-95.

Chen, L., Chen, J., Wu, K., & Yu, L. (2016). Improved low pH emulsification properties of glycated peanut protein isolate by ultrasound Maillard reaction. *Journal of Agricultural and Food Chemistry, 64*(27), 5531-5538.

Chen, W, Ruiling, L., Wang, W., Ma, X., Muhammad, A. L., Guo, M., Ye, X., & Liu, D. (2019). Time effect on structural and functional properties of whey protein isolate-gum acacia conjugates prepared via Maillard reaction. *Journal of the Science of Food and Agriculture,* 99(10), 4801-4807.

Chen, Y., Hu, J., Yi, X., Ding, B., Sun, W., Yan, F., Wei, S., & Li, Z. (2018). Interactions and emulsifying properties of ovalbumin with tannic acid. *LWT-Food Science and Technology,* 95, 282-288.

Corzo-Martínez, M., Moreno, F. J., Olano, A., & Villamiel, M. (2008). Structural characterization of bovine β-lactoglobulin−galactose/tagatose Maillard complexes by electrophoretic, chromatographic, and spectroscopic methods. *Journal of Agricultural and Food Chemistry,* 56(11), 4244-4252.

Davidov-Pardo, G., Perez-Ciordia, S., Marin-Arroyo, MR., & McClements, D. J. (2015). Improving resveratrol bioaccessibility using biopolymer nanoparticles and complexes: impact of protein-carbohydrate Maillard conjugation. *Journal of Agricultural and Food Chemistry,* 63(15), 3915-3923.

Frederico, M. F. B., Christophe, C., Taco, N., Miriam, D. S. L. M., & Lazhar, B. (2018). Effect of the hydrophobicity of fumed silica particles and the nature of

620 oil on the structure and rheological behavior of pickering emulsions. *Journal of*
621 *Dispersion Science and Technology,* 40(8), 1169-1178.

622 Fernandes, R. V. D. B., Silva, E. K., Borges, S. V., Oliveira, C. R. D., Yoshida, M. I.,
623 Silva, Y. F. D., Carmo, E. L.D., Azevedo, V. M., & Botrel, D. A. (2017).
624 Proposing novel encapsulating matrices for spray-dried ginger essential oil from
625 the whey protein isolate-inulin/maltodextrin blends. *Food and Bioprocess*
626 *Technology,* 10(1), 115-130.

627 Goula, A. M., Papatheodorou, A., Karasavva, S., & Kaderides, K. (2016).
628 Ultrasound-assisted aqueous enzymatic extraction of oil from pomegranate seeds.
629 *Waste and Biomass Valorization,* 9(1), 1-11.

630 Habinshuti, I., Chen, X., Yu, J., Mukeshimana, O., Duhoranimana, E., Karangwa, E.,
631 Muhoza, B., Zhang, M., Xia, S., & Zhang, X. (2019). Antimicrobial, antioxidant
632 and sensory properties of maillard reaction products derived from sunflower,
633 soybean and corn meal hydrolysates. LWT-Food Science and Technology, 101,
634 694-702.

635 Han, L., Ratcliffe, I., & Williams, P. A. (2015). Self-assembly and emulsification
636 properties of hydrophobically modified inulin. *Journal of Agricultural and Food*
637 *Chemistry,* 63(14), 3709-3715.

638 Han, L., Ratcliffe, I., & Williams, P. A. (2017). Synthesis, characterisation and
639 physicochemical properties of hydrophobically modified inulin using long-chain
640 fatty acyl chlorides. *Carbohydrate Polymers,* 178, 141-146.

641 Hennessy, A. A., Ross, R. P., Devery, R., & Stanton, C. (2011). The health promoting
642 properties of the conjugated isomers of α-linolenic acid. *Lipids,* 46(2), 105-119.

643 Hu, B., Han, L., Kong, H., Nishinari, K., Phillips, G. O., Yang, J., & Fang, Y. (2019).
644 Preparation and emulsifying properties of trace elements fortified gum arabic.
645 *Food Hydrocolloids,* 88, 43-49.

646 Kristinsson, H. G., & Hultin, H. O. (2003). Effect of low and high pH treatment on

the functional properties of cod muscle proteins. Journal of Agricultural and *Food Chemistry,* 51(17), 5103-5110.

López-Castejón, M. L., Bengoechea, C., Espinosa, S., & Carrera, C. (2019). Characterization of prebiotic emulsions stabilized by inulin and β-lactoglobulin. *Food Hydrocolloids,* 87, 382-393.

Lesmes, U., & McClements, D. J. (2012). Controlling lipid digestibility: Response of lipid droplets coated by β-lactoglobulin-dextran Maillard conjugates to simulated gastrointestinal conditions. *Food Hydrocolloids,* 26(1), 221-230.

Li, Y., Lu, F., Luo, C., Chen, Z., Mao, J., Shoemaker, C., & Zhong, F. (2009). Functional properties of the Maillard reaction products of rice protein with sugar. *Food Chemistry,* 117(1), 69-74.

Liu, J., Liu, W., Salt, L. J., Ridout, M. J., Ding, Y., & Wilde, P. J. (2019). Fish oil emulsions stabilized with caseinate glycated by dextran: physicochemical stability and gastrointestinal fate. *Journal of Agricultural and Food Chemistry,* 67(1), 452-462.

Liu, J., Luo, Y., Gu, S., Xu, Q., Zhang, J., Zhao, P., & Ding, Y. (2017). Physicochemical, conformational and functional properties of silver carp myosin glycated with konjac oligo-glucomannan: Implications for structure-function relationships. *Food Hydrocolloids,* 72, 136-144.

Liu, P., Huang, M., Song, S., Hayat, K., Zhang, X., Xia, S., & Jia, C. (2012). Sensory characteristics and antioxidant activities of Maillard Reaction Products from Soy Protein Hydrolysates with Different Molecular Weight Distribution. *Food and Bioprocess Technology,* 5(5), 1775-1789.

Liu, S., Zhao, P., Zhang, J., Xu, Q., Ding, Y., & Liu, J. (2017). Physicochemical and functional properties of silver carp myofibrillar protein glycated with konjac oligo-glucomannan. *Food Hydrocolloids,* 67, 216-223.

Ma, X., Gao, J., & Chen, H. (2013). Combined effect of glycation and sodium

carbonate-bicarbonate buffer concentration on igG binding, igE binding and conformation of ovalbumin. *Journal of the Science of Food and Agriculture,* 93(13), 3209-3215.

Meerts, I. A. T. M., Verspeek-Rip, C. M., Buskens, C. A. F., Keizer, H. G., Bassaganya-Riera, J., Jouni, Z. E., Huygevoort, A. H. B. M. V., Otterdijk, F. M. V., & Waart, E. J. V. D. (2009). Toxicological evaluation of pomegranate seed oil. *Food and Chemical Toxicology,* 47(6), 1085-1092.

Nooshkam, M., Varidi, M., & Bashash, M. (2019). The Maillard reaction products as food-born antioxidant and antibrowning agents in model and real food systems. *Food Chemistry,* 275, 644-660.

Ozturk, B., & McClements, D. J. (2016). Progress in natural emulsifiers for utilization in food emulsions. *Current Opinion in Food Science,* 7, 1-6.

Rangsansarid, J., Cheetangdee, N., Kinoshita, N., & Fukuda, K. (2008). Bovine serum albumin-sugar conjugates through the Maillard reaction: effects on interfacial behavior and emulsifying ability. *Journal of Oleo Science,* 57(10), 539-547.

Saha, S. S., Chakraborty, A., Ghosh, S., & Ghosh, M. (2012). Comparative study of hypocholesterolemic and hypolipidemic effects of conjugated linolenic acid isomers against induced biochemical perturbations and aberration in erythrocyte membrane fluidity. *European Journal of Nutrition,* 51(4), 483-495.

Sassano, G., Sanderson, P., Franx, J., Groot, P., Straalen, J. V., & Bassaganyariera, J. (2010). Analysis of pomegranate seed oil for the presence of jacaric acid. *Journal of the Science of Food and Agriculture,* 89(6), 1046-1052.

Schaafsma, G., & Slavin, J. L. (2015). Significance of inulin fructans in the human diet. *Comprehensive Reviews in Food Science and Food Safety,* 14(1), 37-47.

Schroder, A., Bertoncarabin, C. C., Venema, P., & Cornacchia, L. (2017). Interfacial properties of whey protein and whey protein hydrolysates and their influence on

O/W emulsion stability. *Food Hydrocolloids,* 73, 129-140.

Sheng, L., Tang, G., Wang, Q., Zou, J., Ma, M., & Huang, X. (2019). Molecular characteristics and foaming properties of ovalbumin-pullulan conjugates through the Maillard reaction. *Food Hydrocolloids,* 100, 105384.

Shi, Y., Liang, R., Chen, L., Liu, H., Goff, H. D., Ma, J., & Zhang, F. (2019). The antioxidant mechanism of Maillard reaction products in oil-in-water emulsion system. *Food Hydrocolloids,* 87, 582-592.

Shah, N. N., Umesh, K. V., & Singhal, R. S. (2019). Hydrophobically modified pea proteins: Synthesis, characterization and evaluation as emulsifiers in eggless cake. *Journal of Food Engineering,* 255, 15-23.

Soleimanian, Y., Goli, S. A. H., Varshosaz, J., & Sahafi, S. M. (2018). Formulation and characterization of novel nanostructured lipid carriers made from beeswax, propolis wax and pomegranate seed oil. *Food Chemistry,* 244, 83-92.

Su, C., Feng, Y., Ye, J., Zhang, Y., Gao, Z., Zhao, M., Yang, N., Nishinari, K., & Fang, Y. (2018). Effect of sodium alginate on the stability of natural soybean oil body emulsions. *RSC Advances,* 8(9), 4731-4741.

Sugumaran, K. R., Gowthami, E., Swathi, B., Elakkiya, S., Srivastava, S. N., Ravikumar, R., Gowdhaman, D. & Ponnusami, V.(2013). Production of pullulan by Aureobasidium pullulans from Asian palm kernel: a novel substrate. *Carbohydrate Polymers,* 92(1), 697-703.

Sun, Y., Hayakawa, S., & Izumori, K., (2004). Modification of ovalbumin with a rare ketohexose through the Maillard reaction: effect on protein structure and gel properties. *Journal of Agricultural and Food Chemistry,* 5(52).

Tang, C., Sun, X., & Foegeding, E. (2011). Modulation of physicochemical and conformational properties of kidney bean vicilin (phaseolin) by glycation with glucose: implications for structure-function relationships of legume vicilins. *Journal of Agricultural and Food Chemistry,* 18(59).

727 Tironi, V. A. , Mabel C Tomás, & María C Añón. (2007). Lipid and protein
728 deterioration during the chilled storage of minced sea salmon. *Journal of the*
729 *Science of Food and Agriculture,* 87(12), 2239-2246.

730 Tong, P., Kasuga, Y., & Khoo, S, C. (2006). Liquid chromatographic-mass
731 spectrometric method for detection of estrogen in commercial oils and in fruit
732 seed oils. *Journal of Food Composition and Analysis,* 19(2-3), 150-156.

733 Wang, Q., Jin, G., Jin, Y., Ma, M., Wang, N., Liu, C., & He, L. (2014). Discriminating
734 eggs from different poultry species by fatty acids and volatiles profiling:
735 Comparison of SPME-GC/MS, electronic nose, and principal component
736 analysis method. *European Journal of Lipid Science and Technology,* 116(8),
737 1044-1053.

738 Wooster, T. J., & Augustin, M. A. (2006). β-Lactoglobulin-dextran Maillard
739 conjugates: Their effect on interfacial thickness and emulsion stability. *Journal*
740 *of Colloid and Interface Science,* 303(2), 564-572.

741 Xie, Y., Jiang, S., & Li, M. (2019). Evaluation on the formation of lipid free radicals
742 in the oxidation process of peanut oil. *LWT-Food Science and Technology,* 104,
743 24-29.

744 Xu, W., & Zhao, X. H. (2019). Structure and property changes of the soy protein
745 isolate glycated with maltose in an ionic liquid through the maillard reaction.
746 *Food and Function,* 10(4), 1948-1957.

747 Xu, X., Liu, W., Liu, C., Luo, L., Chen, J., Luo, S., McClements, D. J., & Wu, L.
748 (2016). Effect of limited enzymatic hydrolysis on structure and emulsifying
749 properties of rice glutelin. *Food Hydrocolloids,* 61, 251-260.

750 Yamasaki, M., Kitagawa, T., Koyanagi, N., Chujo, H. , Maeda, H., Kohno-Murase, J.,
751 Imamura, J., Tachibana, H., Yachibabna, H., & Hirofumi, Y. (2006). Dietary
752 effect of pomegranate seed oil on immune function and lipid metabolism in mice.
753 *Nutrition,* 22(1), 54-59.

754 Yekdane, N., & Goli, S. A. (2019). Effect of Pomegranate Juice on Characteristics and
755 Oxidative Stability of Microencapsulated Pomegranate Seed Oil Using Spray
756 Drying. *Food and Bioprocess Technology*, 12(9), 1614-1625.

757 Zha, F., Dong, S., Rao, J., & Chen, B. (2019). Pea protein isolate-gum arabic maillard
758 conjugates improves physical and oxidative stability of oil-in-water emulsions.
759 *Food Chemistry*, 285, 130-138.

760 Zhang, H., & Rong, T. (2016). Dietary polyphenols, oxidative stress and antioxidant
761 and anti-inflammatory effects. *Current Opinion in Food Science*, 8, 33-42.

762 Zhu, C., Wang, X., & Zhao, X.. (2017). Property modification of caseinate
763 responsible to transglutaminase-induced glycosylation and crosslinking in the
764 presence of a degraded chitosan. *Food Science and Biotechnology*, 24(3),
765 843-850.

766

767

768

Figure Captions:

Figure 1. (a) Conjugation efficiency of OVA glycoconjugates and nonenzymatic browning which was determined by UV/vis absorbance at 420 nm as a function of reaction time; (b) Surface hydrophobicity (H_0) of OVA and glycoconjugates as a function of reaction time. Different letters indicate significant ($P < 0.05$) differences.

Figure 2. (a) Surface tension response to adsorption of OVA and glycoconjugates (2D, 4D, 6D, 8D, and 10D) of OVA at the air/water interface; (b) Far-UV CD spectra of OVA and glycoconjugates (2D, 4D, 6D, 8D, and 10D); (c) Intrinsic fluorescence emission spectra of OVA and glycoconjugates (2D, 4D, 6D, 8D, and 10D); (d) Zeta potentials as a function of pH for OVA and glycoconjugates (2D, 4D, 6D, 8D, and 10D).

Figure 3. DPPH· radical-scavenging activity as a function of reaction time.

Figure 4. Linear plot of adsorption kinetics of OVA and OVA-inulin glycoconjugates with different reaction times (2D, 4D, 6D, 8D, and 10D) at the MCT-water interface at 25□.

Figure 5. (a) Particle size distribution of 20% oil-in-water emulsions prepared using 1.2% OVA and OVA-inulin glycoconjugates with different reaction times (2D, 4D, 6D, 8D, and 10D) after storing at 25℃ for 9 days; (b) Time evolution in D [4,3] of 20% oil-in-water emulsions prepared by using 1.2% OVA and OVA-inulin glycoconjugates with different reaction times (2D, 4D, 6D, 8D, and 10D) after storing at 60℃ for 9 days. Error bars represent the standard deviation of at least two independent replicates. (c) Visual observation of 20% oil-in-water emulsions prepared using 1.2% OVA and OVA-inulin glycoconjugates with different reaction times (2D, 4D, 6D, 8D, and 10D) after storing at 60℃ for 9 days.

Figure 6.(a) pH effect on mean particle diameter D [4,3] and zeta potentials of 20% oil-in-water emulsions prepared using 1.2% OVA and OVA-inulin glycoconjugates with different reaction times (2D, 4D, 6D, 8D, and 10D); (b) Salt effect on zeta potential of 20% oil-in-water emulsions prepared using 1.2% OVA and OVA-inulin glycoconjugates with different reaction times (2D, 4D, 6D, 8D, and 10D) at pH 7; (c) Salt effect on mean particle diameter (D [4,3]) of 20% oil-in-water emulsions

prepared using 1.2% OVA and OVA-inulin glycoconjugates with different reaction times (2D, 4D, 6D, 8D, and 10D) at pH 7.

Figure 7. Peroxide values (PV) of pomegranate seed oil emulsions stabilized by OVA and glycoconjugates (2D, 4D, 6D, 8D, 10D) of OVA at 24 ± 1 °C for 7 days.

Table Captions:

Table 1. Secondary structural compositions, characteristics of native and glycated OVA samples at pH 7.0.

Table 2. The time (T) required to reduce interfacial tension by 30% of the initial value at the pomegranate seed oil-water interface and equilibrium interfacial tension at 7,200 s at 25℃.

Table 3. Fatty acid profile (% total fatty acid) of native and glycated OVA samples analyzed by GC–MS.

Supporting Figure Captions:

Figure S_1. FTIR spectra of OVA and glycoconjugates (2D, 4D, 6D, 8D, and 10D)

Figure S_2. Confocal laser scanning micrographs of the freshly prepared oil-in-water emulsions (OVA, 2D, 4D, 6D, 8D and 10D). Oil droplets were stained with Nile Red and observed under 488 nm, and aqueous phase was stained with Nile Blue and observed under 633 nm (helium neon laser). The micrographs were excited for Nile Red, Nile Blue A and over laps, respectively.

Figure S_3. Transmission electron micrographs (TEM) of the freshly prepared oil-in-water emulsions (OVA, 2D, 4D, 6D, 8D and 10D).

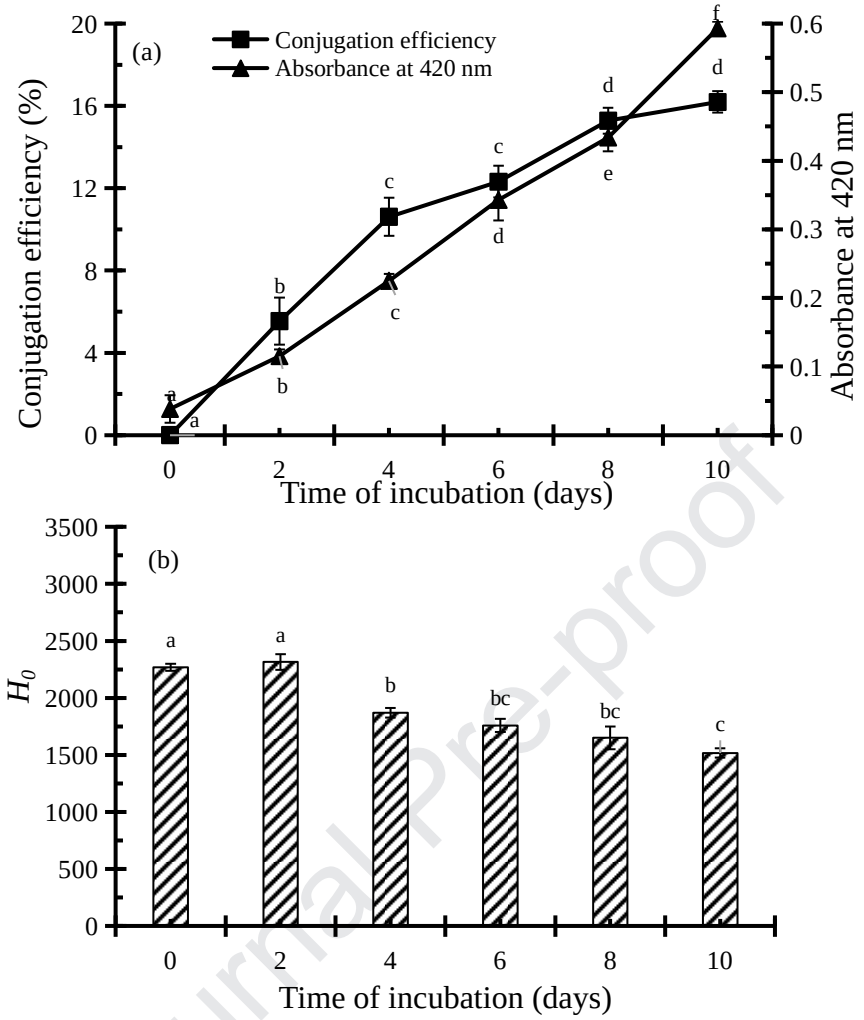

Figure 1. (a) Conjugation efficiency of OVA glycoconjugates and nonenzymatic browning which was determined by UV/vis absorbance at 420 nm as a function of reaction time; (b) Surface hydrophobicity (H_0) of OVA and glycoconjugates as a function of reaction time. Different letters indicate significant ($P < 0.05$) differences.

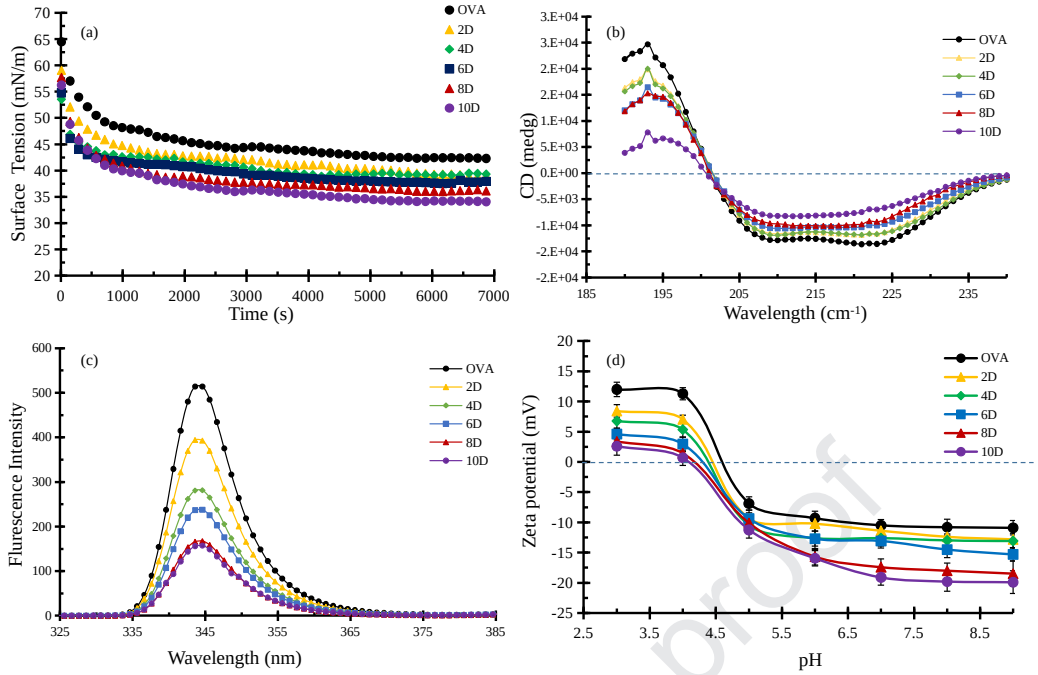

Figure 2. (a) Surface tension response to adsorption of OVA and glycoconjugates (2D, 4D, 6D, 8D, and 10D) of OVA at the air/water interface; (b) Far-UV CD spectra of OVA and glycoconjugates (2D, 4D, 6D, 8D, and 10D); (c) Intrinsic fluorescence emission spectra of OVA and glycoconjugates (2D, 4D, 6D, 8D, and 10D); (d) Zeta potentials as a function of pH for OVA and glycoconjugates (2D, 4D, 6D, 8D, and 10D).

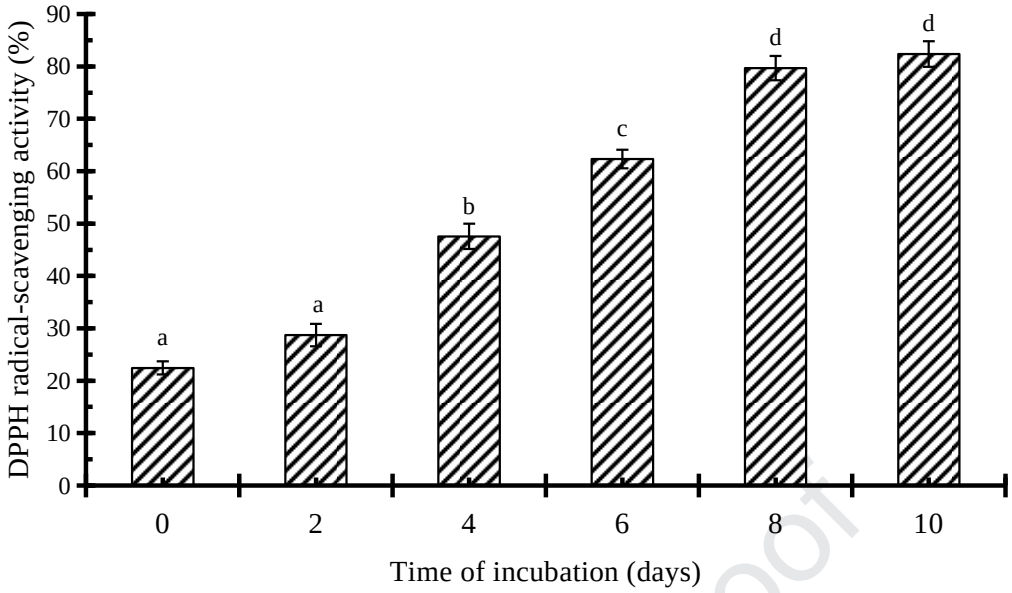

839

840 **Figure 3.** DPPH· radical-scavenging activity as a function of reaction time.

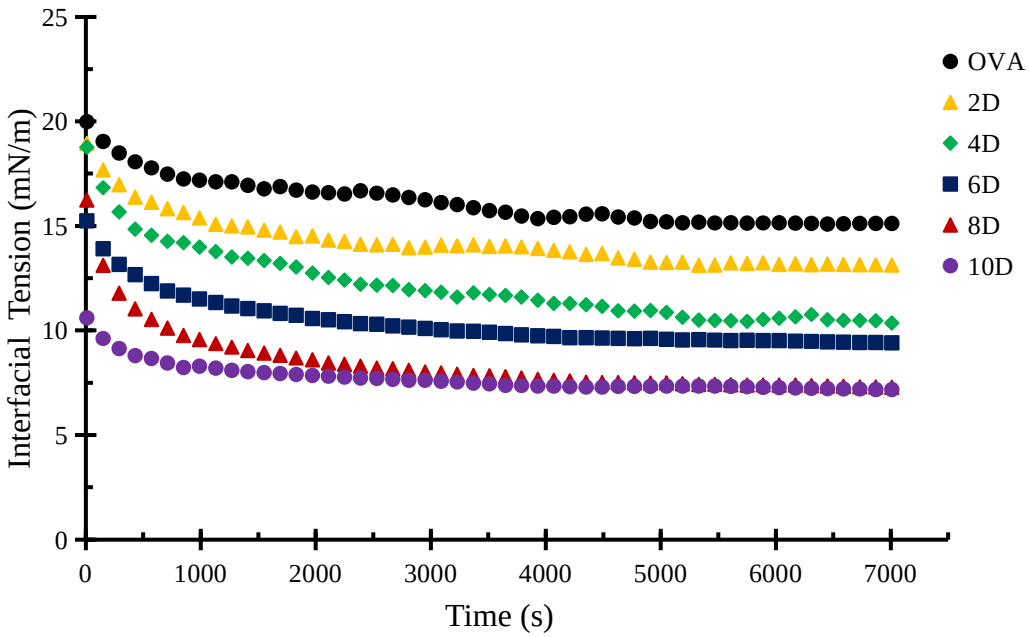

841

842 **Figure 4.** Linear plot of adsorption kinetics of OVA and OVA-inulin glycoconjugates
843 with different reaction times (2D, 4D, 6D, 8D, and 10D) at the pomegranate seed
844 oil-water interface at 25□.

845

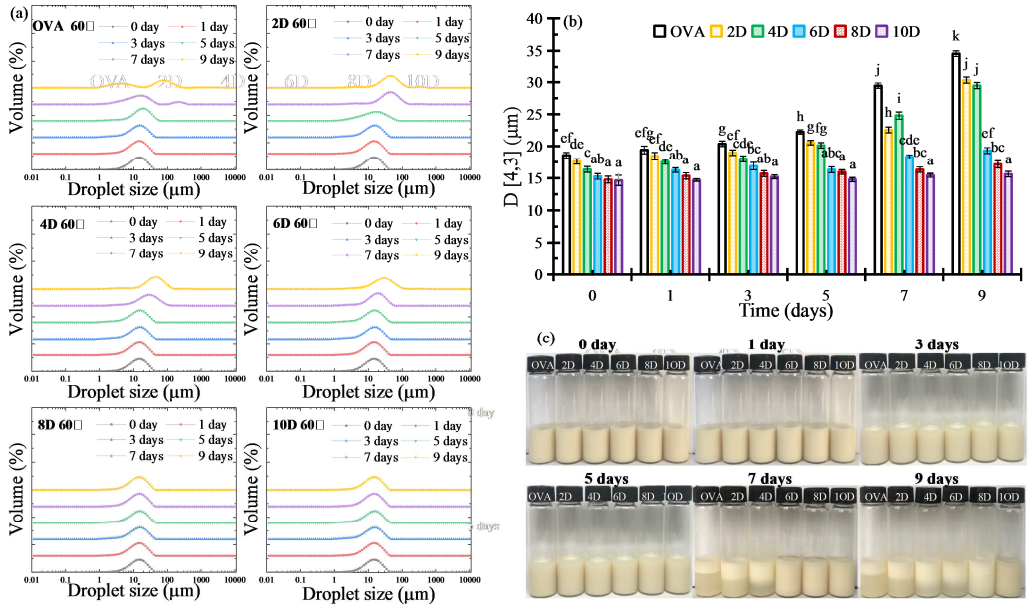

Figure 5. (a) Particle size distribution of 20% oil-in-water emulsions prepared using 1.2% OVA and OVA-inulin glycoconjugates with different reaction times (2D, 4D, 6D, 8D, and 10D) after storing at 60℃ for 9 days; (b) Time evolution in D [4,3] of 20% oil-in-water emulsions prepared by using 1.2% OVA and OVA-inulin glycoconjugates with different reaction times (2D, 4D, 6D, 8D, and 10D) after storing at 60℃ for 9 days. Error bars represent the standard deviation of at least two independent replicates. (c) Visual observation of 20% oil-in-water emulsions prepared using 1.2% OVA and OVA-inulin glycoconjugates with different reaction times (2D, 4D, 6D, 8D, and 10D) after storing at 60℃ for 9 days.

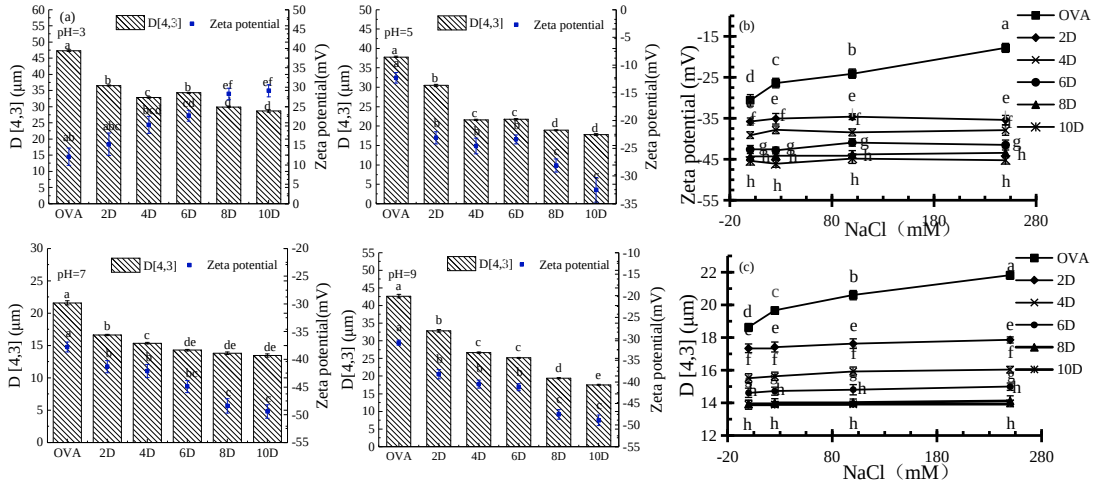

Figure 6. (a) pH effect on mean particle diameter D [4,3] and zeta potential of 20% oil-in-water emulsions prepared using 1.2% OVA and OVA-inulin glycoconjugates with different reaction times (2D, 4D, 6D, 8D, and 10D); (b) Salt effect on zeta potentials of 20% oil-in-water emulsions prepared using 1.2% OVA and OVA-inulin glycoconjugates with different reaction times (2D, 4D, 6D, 8D, and 10D) at pH 7; (c) Salt effect on mean particle diameter (D [4,3]) of 20% oil-in-water emulsions prepared using 1.2% OVA and OVA-inulin glycoconjugates with different reaction times (2D, 4D, 6D, 8D, and 10D) at pH 7.

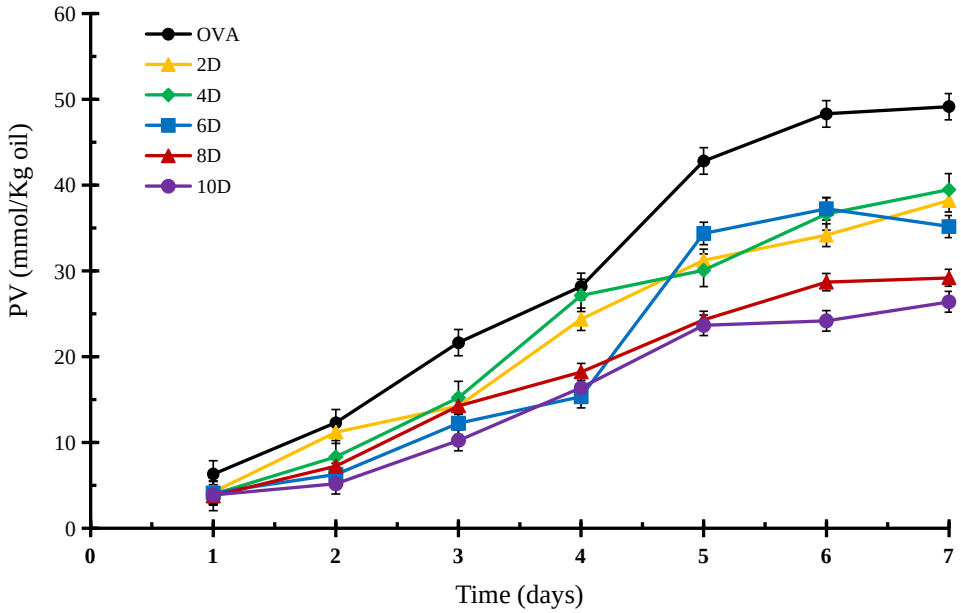

Figure 7. Peroxide values (PV) of pomegranate seed oil emulsions stabilized by OVA and glycoconjugates (2D, 4D, 6D, 8D, 10D) of OVA at 24 ± 1 °C for 7 days.

876 Table 1. Secondary structural compositions, characteristics of native and glycated
877 OVA samples at pH 7.0.

Samples		Secondary structure composition (%)			
Molar ratio	Reaction period (days)	α-Helix [a]	β-Sheet [b]	Turns	Random coil
native	0	38.2	16.85	16.1	28.9
	2	36.4	24.3	12.1	27.2
	4	36.6	23.0	12.3	28.2
1:4	6	30.6	29.9	11.3	28.3
	8	31.0	37.8	6.2	25.0
	10	22.8	45.3	8.4	23.5

878 a Combined regular and distorted α-helix.

879 b Combined regular and distorted β-sheets.

880

881 Table 2. The time (T) required to reduce interfacial tension by 30% of the initial value
882 at the pomegranate seed oil-water interface and equilibrium interfacial tension at
883 7,200 s at 25□.

Solution sample	T (s)	Equilibrium interfacial (mN/m)
OVA	1332	15.12
2D	1129	13.11
4D	849	10.33
6D	709	9.39
8D	549	7.27
10D	429	7.13

884

885 Table 3. Fatty acid profile (% total fatty acid) of pomegranate seed oil emulsions
886 stabilized by OVA and glycoconjugates (2D, 4D, 6D, 8D, 10D) of OVA at 60 ± 1 °C
887 for 7 days.

Fatty aicd(%)	Initial oil	Bulk oil	OVA	2D	4D	6D	8D	10D
	0 day	7 days						
Palmitic C16:0 (%)	2.99±0.05[a]	5.31±0.03[d]	5.12±0.01[d]	4.76±0.06[c]	5.37±0.02[d]	4.55±0.03[c]	3.63±0.01[b]	3.42±0.04[b]
Stearic C18:0 (%)	2.45±0.03[a]	5.21±0.02[d]	5.08±0.01[d]	4.85±0.01[c]	4.63±0.01[c]	3.24±0.01[b]	3.05±0.02[b]	2.89±0.02[b]
Oleic C18:1 (%)	5.94±0.01[b]	6.24±0.04[c]	6.01±0.02[b]	7.01±0.02[e]	6.59±0.03[d]	5.21±0.02[a]	5.68±0.02[b]	5.30±0.01[a]
Linoleic C18:2 (%)	6.88±0.01[a]	7.36±0.03[c]	7.03±0.03[b]	6.82±0.03[a]	6.77±0.04[a]	6.92±0.01[a]	6.87±0.01[a]	6.68±0.01[a]
Linolenic C18:3 (%)	76.3±0.02[d]	68.2±0.04[a]	69.1±0.02[a]	70.3±0.02[b]	69.5±0.03[a]	71.4±0.04[c]	72.6±0.02[c]	73.1±0.02[c]
Arachidic C20:0 (%)	4.36±0.03[a]	4.42±0.01[a]	4.40±0.02[a]	4.54±0.01[a]	4.47±0.02[a]	4.50±0.06[a]	4.43±0.03[a]	4.48±0.03[a]
SFA (%)	9.80±0.06[a]	14.9±0.02[d]	14.6±0.01[d]	14.2±0.01[d]	14.5±0.01[a]	12.3±0.04[c]	11.1±0.04[b]	10.8±0.04[a]
UFA (%)	89.1±0.11[a]	71.8±0.07[d]	75.1±0.06[d]	84.1±0.05[d]	82.8±0.04[a]	84.4±0.03[c]	86.1±0.04[b]	89.8±0.07[a]
MUFA (%)	5.94±0.02[b]	6.24±0.03[c]	6.01±0.02[c]	7.01±0.02[e]	6.59±0.02[d]	5.21±0.01[a]	5.68±0.03[b]	5.30±0.03[a]
PUFA (%)	83.2±0.04[d]	75.6±0.02[b]	69.1±0.05[a]	77.1±0.04[b]	76.3±0.03[b]	79.2±0.03[c]	81.3±0.01[c]	81.5±0.02[c]

888 [a,b,c,d,e] fronts mean ranking in all treatment groups by Duncan's Multiple Range Tests.
889 Values are mean ± SD, n = 3
890 *SFA* saturated fatty acid, *UFA* unsaturated fatty acid, *MUFA* monounsaturated fatty
891 acid, *PUFA* polyunsaturated fatty acid, . The fatty acid data exhibited significant
892 difference ($p < 0.05$).
893
894
895
896
897
898
899

900 Supporting Information

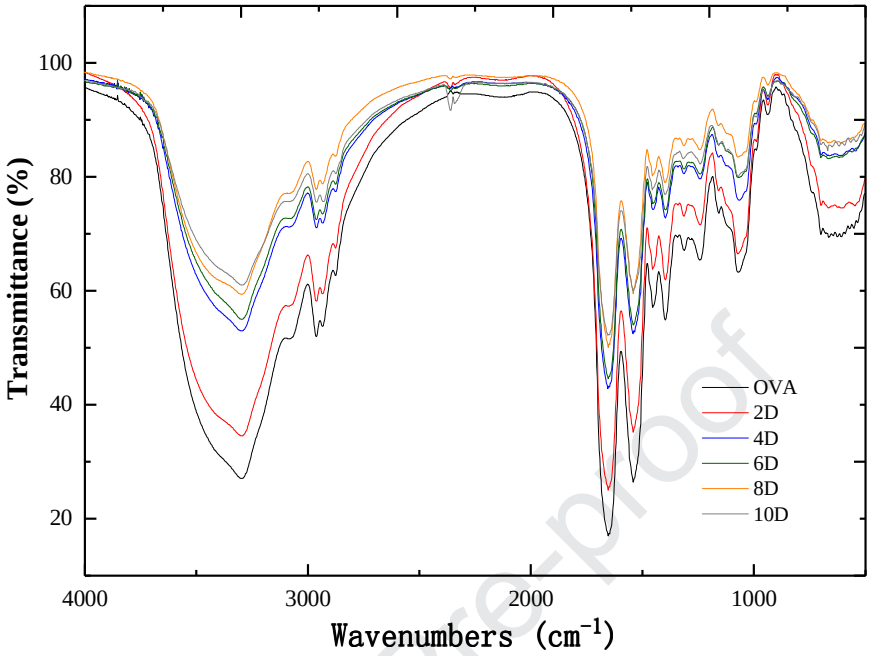

901

902 **Figure S_1.** FTIR spectra of OVA and glycoconjugates (2D, 4D, 6D, 8D, and 10D)

903

904

905

906

907

908

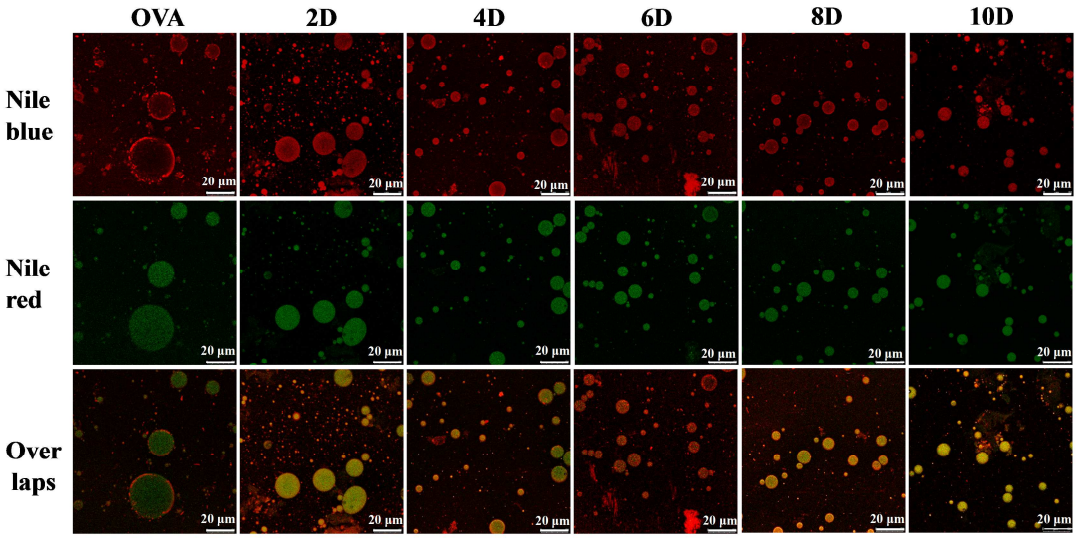

Figure S_2. Confocal laser scanning micrographs of the freshly prepared oil-in-water emulsions (OVA, 2D, 4D, 6D, 8D and 10D). Oil droplets were stained with Nile Red and observed under 488 nm, and aqueous phase was stained with Nile Blue and observed under 633 nm (helium neon laser). The micrographs were excited for Nile Red, Nile Blue A and over laps, respectively.

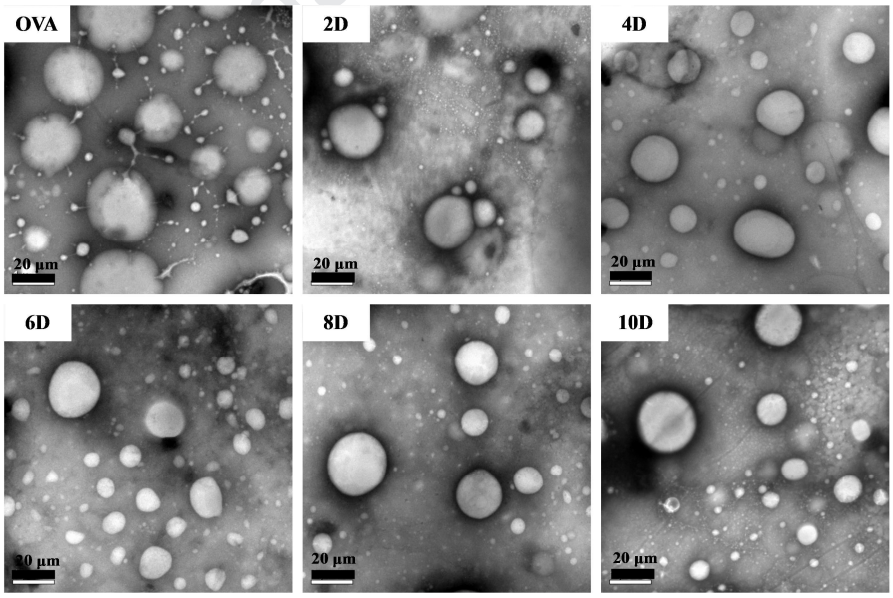

Figure S_3. Transmission electron micrographs (TEM) of the freshly prepared oil-in-water emulsions (OVA, 2D, 4D, 6D, 8D and 10D).

Highlights

1) OVA glycosylates with inulin showed a better emulsifying activity.
2) The OVA-inulin emulsion could prevent pomegranate seed oil from oxidation.
3) OVA-inulin can greatly extend the range of pH values at which they remain stable.
4) OVA glycosylates with inulin clearly show improving the salt stability.

Conflicts of Interest

There are no conflicts of interest to declare.